2010 IEEE International Conference on Robotics and Automation
Anchorage Convention District
May 3-8, 2010, Anchorage, Alaska, USA

Out-of-Plane Orbit Estimation and Tracking for Aerial Recovery of Micro Air Vehicles

Daniel C. Carlson and Mark B. Colton, *Member, IEEE*

***Abstract*— Aerial recovery of autonomous micro air vehicles (MAVs) presents many unique challenges due to the difference in size and speed of the recovery vehicle and MAV. This paper presents algorithms to enable an autonomous MAV to estimate the orbit of a recovery vehicle and track the orbit until the final docking phase. Several algorithms are presented, which are shown to be robust and computationally inexpensive. Methods for estimating ellipses that are rotated out of the x-y plane are developed and demonstrated through simulation. An algorithm to enable the MAV to track the recovery vehicle's orbit, based on the vector field approach, is also presented.**

I. Introduction

In recent years unmanned air vehicles (UAVs) have become increasingly important in modern warfare. Certain large UAVs have high-altitude, long-endurance intelligence, surveillance and reconnaissance (ISR) capabilities, whereas micro air vehicles (MAVs) are better suited for short-term, low-altitude ISR missions. Backpackable MAVs can be carried and launched by a common soldier to provide time-critical ISR. Due to their limited range, retrieving MAVs is problematic in certain applications. One recovery method is for ground forces to retrieve the MAV after the completion of the mission. This, however, is potentially dangerous because a landing MAV may reveal the location of the forces, who must by necessity be in the vicinity of the MAV. Another solution is for the MAV to return to a distant base, but MAVs are often deployed deep in enemy territory and lack sufficient range to return to base.

The approach taken in this paper is to use a larger aircraft, either manned or unmanned, for in-flight recovery of MAVs. A major challenge with this solution is the high speed of the large aircraft relative to that of the MAV, making gentle retrieval using methods similar to those employed for mid-air fueling unfeasible. Additionally, large aircraft generate significant regions of turbulence ("wash") from their engines and air flow around their wings and fuselage. This wash can cause major disturbances to a MAV trying to dock with a significantly larger vehicle. Due to these challenges, aerial recovery of MAVs is problematic and has not been previously implemented. The purpose of this paper is to describe methods that will make possible the autonomous aerial recovery of MAVs using a larger, faster recovery vehicle.

A. Aerial Recovery Concept

Our method of aerial recovery is illustrated in Figure 1. In this method, a towplane ("mothership") tows a smaller drogue that is used as a docking station for the MAV. As shown in references [1], [2], a large, relatively fast orbit of the mothership results in a smaller, slower orbit of the drogue. Skop and Choo show that for a sufficiently long cable and with sufficient drag, the radius of the drogue orbit will approach zero. In our method of aerial recovery, the mothership executes an orbit such that the speed of the drogue is slightly lower than the nominal speed of the MAV, and the radius of the drogue orbit is larger than the minimum turn radius of the MAV. This allows the MAV to enter the orbit of the drogue, approach it from behind at a relatively low closing speed, and gently dock with the drogue. The problem of the large difference in speeds between the mothership and MAV is therefore overcome by enabling docking between the MAV and the slower drogue.

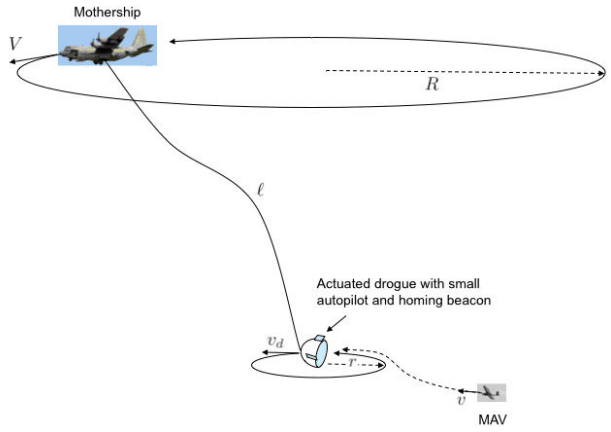

Fig. 1. Aerial recovery concept. The mothership tows a drogue, which executes a relatively slow orbit to facilitate MAV-drogue docking.

There are three critical components in this research. First, the dynamics of the mothership-drogue system must be modeled. Specifically, the forward and inverse dynamics of the mothership-drogue system are needed for simulation and control, respectively [3], [4], [5]. This first component of this research has been considered previously [6]. Second, estimation and control algorithms must be developed that enable autonomous cooperative docking between the MAV and the drogue. Third, the drogue and towing system must be designed to achieve the desired aerodynamic properties and to enable consistent and robust retrieval of the MAV.

This paper focuses on the algorithms that enable a MAV to estimate and enter the orbit of the drogue in preparation for final rendezvous and docking. By estimating and tracking the orbit of the drogue, the attitudes and velocities of the vehicles will be similar as the MAV approaches the drogue, thus facilitating docking. For this work, it is assumed that there is

communication between the drogue and MAV, allowing the drogue to transmit its position and heading (from an on-board GPS receiver) to the MAV. The drogue orbit is estimated from the transmitted data and a coordinated rendezvous approach is taken, rather than treating the drogue as a target during the initial stages of rendezvous. During the final stages of rendezvous, when the distance between the MAV and drogue is small compared to the error of the orbit estimate, it is necessary to use some other rendezvous algorithm (e.g., vision-based proportional navigation) [7]. This paper focuses on the problem of estimating the drogue orbit from GPS data and tracking that orbit until the point when vision-based rendezvous is required. The algorithms for the final docking will be addressed in future work.

In this paper we assume that the drogue follows an elliptical orbit. Ideally, the drogue will travel in a circular orbit in a plane parallel to the ground. In practice, the actual drogue orbit is not circular and is not restricted to the horizontal plane due to 1) wind and other disturbances, 2) unmodeled mothership-drogue dynamics, and 3) the numerical approximations inherent in the inverse dynamics to find the required mothership orbit from the desired circular drogue orbit. Additionally, initial flight tests demonstrate that an ellipse is an appropriate model [8]. Consequently, for estimation purposes, the drogue orbit will be treated as an ellipse. In Section II we present methods for estimating the parameters of an elliptical orbit that is in the horizontal plane. In Section III we extend the work to the case of an elliptical orbit that is arbitrarily rotated out of the horizontal plane. In Section IV we present methods that enable the MAV to track the estimated drogue orbit.

II. In-Plane Orbit Estimation

The parametric equations for an elliptical orbit in the horizontal (x-y) plane are given by

$$\begin{aligned} x - x_0 &= a\cos(t)\cos(\psi) - b\sin(t)\sin(\psi) \\ y - y_0 &= a\cos(t)\sin(\psi) + b\sin(t)\cos(\psi), \end{aligned} \tag{1}$$

where t is time, x_0 and y_0 are the coordinates of the center of the ellipse, a and b are the major and minor axes, respectively, and ψ is the angle of rotation of the ellipse in the horizontal plane, measured from the x-axis. An ellipse may also be represented using the general equation of a conic,

$$F(x,y) = a_1x^2 + a_2xy + a_3y^2 + a_4x + a_5y + a_6 = 0, \tag{2}$$

where a_i, $i = 1...6$ are the conic parameters. The objective is to estimate these parameters from N measurements of the drogue's x and y GPS coordinates, which can be accomplished using least squares regression. The resulting parameters may be converted to the parameters that describe an ellipse in parametric form, as defined by (1).

A. Fitzgibbon's Method

The disadvantage of the method just described is that the parameters estimated in this way are not guaranteed to represent an ellipse; since (2) is the equation for general conics, the estimated parameters may instead represent parabolic or hyperbolic trajectories. Fitzgibbon proposed a method in which an ellipse-specific constraint is used to guarantee that the solution represents an ellipse [9]. For (2) to represent an ellipse, the parameters are constrained by

$$4a_1a_3 - a_2^2 > 0. \tag{3}$$

It has been shown that recasting this as an equality constraint, in which (3) is still satisfied, results in valid parameter estimates whose values are not dependent on the particular constant value used on the right side of (3) [9]. Essentially, since (3) can be multiplied by a constant and the result is the same ellipse, equation (3) can be set to an arbitrary constant without loss of generality. Thus the constraint can be written, without loss of generality, as

$$4a_1a_3 - a_2^2 = 1.$$

Equation (2) can be written in matrix form as

$$F(\mathbf{x}) = \mathbf{x}\cdot\mathbf{a}$$

where

$$\mathbf{a} = \begin{bmatrix} a_1 & a_2 & a_3 & a_4 & a_5 & a_6 \end{bmatrix}^T \tag{4}$$

and

$$\mathbf{x} = \begin{bmatrix} x^2 & xy & y^2 & x & y & 1 \end{bmatrix}.$$

Determining the conic parameters is equivalent to minimizing the distance from all of the points to the conic,

$$\min_{\mathbf{a}} \sum_{i=1}^{N} (\mathbf{x_i}\cdot\mathbf{a})^2 \text{ subject to } 4a_1a_3 - a_2^2 = 1,$$

or, in matrix form, as

$$\min_{\mathbf{a}} \|\mathbf{Da}\|^2 \text{ subject to } \mathbf{a^TCa} = 1, \tag{5}$$

where

$$\mathbf{D} = \begin{bmatrix} x_1^2 & x_1y_1 & y_1^2 & x_1 & y_1 & 1 \\ \vdots & \vdots & \vdots & \vdots & \vdots & \vdots \\ x_N^2 & x_Ny_N & y_N^2 & x_N & y_N & 1 \end{bmatrix},$$

and

$$\mathbf{C} = \begin{bmatrix} 0 & 0 & 2 & 0 & 0 & 0 \\ 0 & -1 & 0 & 0 & 0 & 0 \\ 2 & 0 & 0 & 0 & 0 & 0 \\ 0 & 0 & 0 & 0 & 0 & 0 \\ 0 & 0 & 0 & 0 & 0 & 0 \\ 0 & 0 & 0 & 0 & 0 & 0 \end{bmatrix}.$$

$\mathbf{D}$ therefore contains the N measured drogue locations and $\mathbf{C}$ describes the ellipse constraint. Equation (5) describes a quadratically constrained least squares minimization problem. By applying Lagrange multipliers, this equation can

be solved using a method proposed by Gander [10], which recasts (5) as

$$\mathbf{Sa} = \lambda \mathbf{Ca} \text{ subject to } \mathbf{a^T Ca} = 1, \tag{6}$$

where $\mathbf{S} = \mathbf{D^T D}$. Solving (6) yields six possible solutions for $\mathbf{a}$; the correct least-squares solution is the eigenvector that corresponds to the smallest positive eigenvalue.

B. Numerically Stable Improvement

Fitzgibbon's method has the drawback that the computation of the eigenvalues is sometimes unstable and can yield infinite or complex results. This arises from the fact that $\mathbf{D}^T\mathbf{D}$ is often nearly singular. Halir and Flusser [11] proposed a method for improving the accuracy and speed of the algorithm. This method makes use of the special structure of the matrices to eliminate the singularities. The result is unstable only if all of the points lie on the same line, in which case there is no suitable approximation for an ellipse. In this method $\mathbf{D}$ is restructured as $\mathbf{D} = \begin{pmatrix} \mathbf{D_1} & \mathbf{D_2} \end{pmatrix}$, where

$$\mathbf{D_1} = \begin{bmatrix} x_1^2 & x_1y_1 & y_1^2 \\ \vdots & \vdots & \vdots \\ x_i^2 & x_iy_i & y_i^2 \\ \vdots & \vdots & \vdots \\ x_N^2 & x_Ny_N & y_N^2 \end{bmatrix}, \mathbf{D}_2 = \begin{bmatrix} x_1 & y_1 & 1 \\ \vdots & \vdots & \vdots \\ x_i & y_i & 1 \\ \vdots & \vdots & \vdots \\ x_N & y_N & 1 \end{bmatrix}.$$

S, C, and **a** are also restructured:

$$\mathbf{S} = \begin{bmatrix} S_1 & S_2 \\ S_2^T & S_3 \end{bmatrix} \text{ where } \begin{array}{l} \mathbf{S_1} = \mathbf{D_1^T D_1} \\ \mathbf{S_2} = \mathbf{D_1^T D_2} \\ \mathbf{S_3} = \mathbf{D_2^T D_2} \end{array}$$

$$\mathbf{C} = \begin{bmatrix} \mathbf{C_1} & \mathbf{0} \\ \mathbf{0} & \mathbf{0} \end{bmatrix} \text{ where } \mathbf{C}_1 = \begin{bmatrix} 0 & 0 & 2 \\ 0 & -1 & 0 \\ 2 & 0 & 0 \end{bmatrix}$$

$$\mathbf{a} = \begin{bmatrix} \mathbf{a_1} \\ \mathbf{a_2} \end{bmatrix} \text{ where } \mathbf{a_1} = \begin{bmatrix} a \\ b \\ c \end{bmatrix} \text{ and } \mathbf{a_2} = \begin{bmatrix} d \\ e \\ f \end{bmatrix}.$$

Equation (6) then becomes

$$\begin{bmatrix} \mathbf{S_1} & \mathbf{S_2} \\ \mathbf{S_2^T} & \mathbf{S_3} \end{bmatrix} \cdot \begin{bmatrix} \mathbf{a_1} \\ \mathbf{a_2} \end{bmatrix} = \lambda \cdot \begin{bmatrix} \mathbf{C_1} & \mathbf{0} \\ \mathbf{0} & \mathbf{0} \end{bmatrix} \cdot \begin{bmatrix} \mathbf{a_1} \\ \mathbf{a_2} \end{bmatrix},$$

which is used to solve for the parameters in vectors $\mathbf{a}_1$ and $\mathbf{a}_2$.

C. Recursive Least Squares

The method introduced by Halir and Flusser is used to obtain an estimate of orbit parameters from the first N GPS data points provided by the drogue. As new GPS data become available during the course of the aerial recovery process, it is computationally expensive to continue to use the method just described to update the orbit estimates because the size of $\mathbf{D}$ continues to increase with each new data point. Instead, recursive least squares (RLS) [12] is used to update the estimate for each new GPS data point received from the drogue. The parameters to estimate are again represented by the vector $\mathbf{a}$ defined in (4). The parameter estimates are updated using

$$\gamma_{n+1} = \frac{1}{\lambda + \mathbf{x}_{n+1}^T \mathbf{P}_n \mathbf{x}_{n+1}}$$

$$\mathbf{a}_{n+1} = \mathbf{a}_n - \gamma_{n+1} \mathbf{P}_n \mathbf{x}_{n+1} \mathbf{x}_{n+1}^T \mathbf{a}_n$$

$$\mathbf{P}_{n+1} = \frac{1}{\lambda} \left(\mathbf{P}_n - \gamma_{n+1} \mathbf{P}_n \mathbf{x}_{n+1} \mathbf{x}_{n+1}^T \mathbf{P}_n \right)$$

The matrix $\mathbf{P}$ (the Grammian) is initialized to the identity matrix. The vector $\mathbf{x}$ represents a vector of the most recent GPS data received from the drogue, and λ is the forgetting factor, which is a tunable parameter that controls the responsiveness of the estimates and the level of filtering, with higher λ values resulting in smoother but less-responsive parameter estimates.

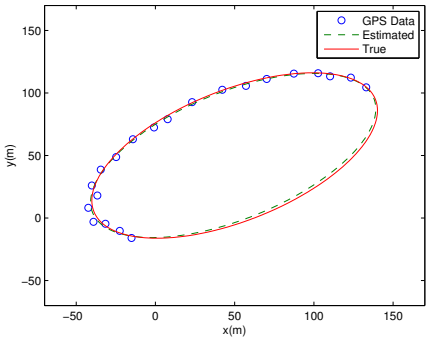

Fig. 2. Estimated drogue orbit from simulated noisy data.. The solid line represents the true orbit. The circles represent simulated noisy GPS data points. The dashed line represents the estimated drogue orbit.

D. Simulation Results

The Halir-Flusser method followed by RLS was applied to simulated GPS data from the drogue, with additive Gaussian noise with a standard deviation of 5 m to simulate uncertainty in the GPS measurement. Figure 2 shows the resulting estimated elliptical orbit. Figure 3 shows the evolution of the estimate of x_0 (the north position of the center of the ellipse) as new GPS data points are included in the recursion. It is clear that the estimate converges to the true value of 50 m. Figure 3 also shows the evolution of the estimate of the ellipse major axis. Again, the estimate converges to the true value. Estimates for the other ellipse parameters (minor axis, rotation angle, and east location of the center) follow similar trends.

III. Out-of-Plane Orbit Estimation

As mentioned in Section I-A, the drogue orbit will, in general, not be perfectly aligned with the horizontal plane. This, in fact, has been observed in initial experiments to validate the mothership-drogue dynamic model [6]. The

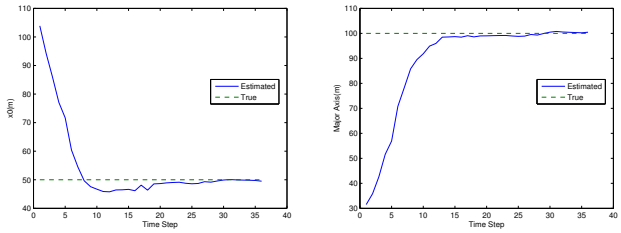

Fig. 3. Estimate of x_0 and major axis using Halir-Flusser method and RLS.

purpose of this section is to extend the methods of Section II, by which elliptical orbits in the horizontal plane may be estimated, to the more general problem of estimating arbitrarily rotated, out-of-plane elliptical orbits.

A. Methods

An ellipse in 3-space is described by eight parameters,

$$\{(x, y, z) \mid f(x_0, y_0, z_0, a, b, \psi_1, \theta, \psi_2) = 0\},$$

where x_0, y_0, and z_0 describe the center of the ellipse, a and b are the major and minor axes, respectively, and ψ_1, θ, and ψ_2 are 3-2-3 Euler angles describing the rotation of the ellipse [13]. With the added degrees of freedom, estimating the ellipse becomes significantly more difficult. The approach taken in this paper is to estimate the plane on which the points describing the ellipse lie. The normal vector describing that plane gives information about θ and ψ_1. The measured ellipse points are transformed into the coordinate frame describing the plane (the "ellipse frame"), and the ellipse parameters are estimated in the manner that was developed in Section II.

The transformation from the inertial frame to the ellipse frame is given by $R = R_{\psi_2} R_\theta R_{\psi_1}$, where $R_{\psi_1}$is a rotation about the inertial z axis, R_θ is a rotation about the y axis of the first intermediate frame, and R_{ψ_2} is a rotation about the z axis of the second intermediate frame. The parametric form for an ellipse described in the inertial frame is given by

$$\begin{bmatrix} x - x_0 \\ y - y_0 \\ z - z_0 \end{bmatrix} = R_{\psi_1}^T R_\theta^T R_{\psi_2}^T \begin{bmatrix} a\cos(t) \\ b\sin(t) \\ 0 \end{bmatrix}.$$

The plane on which the ellipse points lie can be described in vector form as $\mathbf{db} = \mathbf{0}$, where $\mathbf{d} = \begin{bmatrix} x & y & z & 1 \end{bmatrix}$ and $\mathbf{b} = \begin{bmatrix} b_1 & b_2 & b_3 & b_4 \end{bmatrix}^T$. For N measurements of the drogue position, the equation describing the orbit plane becomes $\mathbf{Db} = \mathbf{0}$, where

$$\mathbf{D} = \begin{bmatrix} x_1 & y_1 & z_1 & 1 \\ \vdots & \vdots & \vdots & \vdots \\ x_N & y_N & z_N & 1 \end{bmatrix}.$$

Using Singular Value Decomposition (SVD) [12] the equation can be written as $\mathbf{U\Lambda V}^T\mathbf{b} = \mathbf{0}$. The column of $\mathbf{V}$ that corresponds to the smallest singular value is the solution vector containing the plane parameters $\mathbf{b}$. The plane's normal vector, $\mathbf{n} = \begin{bmatrix} n_x & n_y & n_z \end{bmatrix}$, can then be calculated from

$$\begin{aligned} n_x &= \frac{b_1}{\sqrt{b_1^2+b_2^2+b_3^2}} \\ n_y &= \frac{b_2}{\sqrt{b_1^2+b_2^2+b_3^2}} \\ n_z &= \frac{b_3}{\sqrt{b_1^2+b_2^2+b_3^2}} \end{aligned}.$$

The normal vector can be written in the ellipse frame as $\begin{bmatrix} 0 & 0 & 1 \end{bmatrix}^T$, and related to inertial frame using

$$\begin{bmatrix} 0 \\ 0 \\ 1 \end{bmatrix} = R_{\psi_2} R_\theta R_{\psi_1} \begin{bmatrix} n_x \\ n_y \\ n_z \end{bmatrix}.$$

The angle ψ_1 can then be calculated from

$$\tan\psi_1 = \frac{n_y}{n_x},$$

and the normal vector is expressed in the first intermediate frame as $\mathbf{n}' = R_{\psi_1}\mathbf{n}$. The angle θ is calculated from

$$\tan\theta = \frac{n_x'}{n_z'}.$$

All data points can now be converted into the ellipse frame using

$$\begin{bmatrix} x'' \\ y'' \\ z'' \end{bmatrix} = R_\theta R_{\psi_1} \begin{bmatrix} x \\ y \\ z \end{bmatrix},$$

and the remaining parameters a, b, x_0'', y_0'', ψ_2 are estimated using Halir's method as described in Section II-B, where x_0'' and y_0'' are the center of the ellipse in the ellipse frame. Finally, x_0'' and y_0'' can be transformed into the inertial frame using

$$\begin{bmatrix} x_0 \\ y_0 \\ z_0 \end{bmatrix} = R_{\psi_1}^T R_\theta^T \begin{bmatrix} x_0'' \\ y_0'' \\ z_0'' \end{bmatrix}.$$

where z_0'' is 0.

After using these methods to obtain initial estimates of the normal vector and ellipse parameters, RLS is again employed to update the estimates as new drogue measurements become available. The RLS algorithm is applied twice. First, it is used to update the estimate of the normal vector that describes the plane on which all the measurements lie. Second, the most recent measurement is rotated into that frame and RLS is used to update the ellipse parameter estimates.

B. Simulation Results

Figure 4 shows a 3D plot of the out-of-plane ellipse estimation results. Figure 5 shows the evolution of the estimate of x_0 and of the Euler angle θ. Results for the other parameters show similar trends.

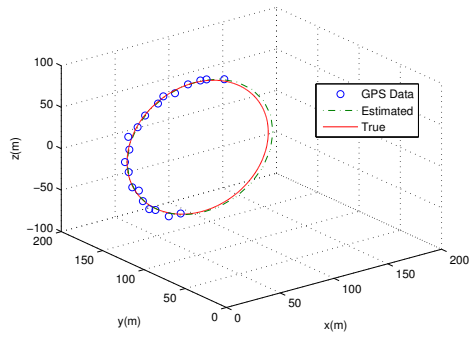

Fig. 4. Estimated out-of-plane drogue orbit from simulated noisy data.

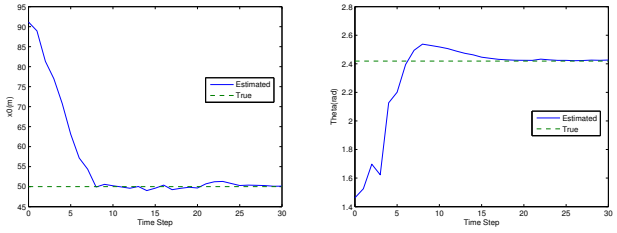

Fig. 5. Estimate of x_0 and θ for an out-of-plane orbit.

IV. Orbit Tracking

In order to match the attitudes and velocities of the drogue and MAV, the MAV inserts itself onto the drogue orbit at a point behind the drogue, and then tracks the orbit at a speed slightly higher than that of the drogue until rendezvous occurs. This section describes methods that enable the MAV to enter and track the drogue orbit. The control approach taken in this work is to decouple lateral control (for horizontal tracking) from longitudinal control (for altitude tracking). The horizontal orbit is the elliptical projection of the drogue orbit onto the horizontal plane, which is estimated using the methods described in Sections II and III.

A. Lateral Control

The lateral control to achieve elliptical orbit tracking of the MAV is done using a vector field method based on the work done by Barber, but it is expanded to tracking of ellipses in addition to circles [14]. First, the coordinate frame is rotated so that there is no rotation of the ellipse from the x axis. This transformation is done using the rotation matrix

$$R_{\psi_2} = \begin{bmatrix} \cos\psi_2 & \sin\psi_2 & 0 \\ -\sin\psi_2 & \cos\psi_2 & 0 \\ 0 & 0 & 1 \end{bmatrix},$$

where ψ_2 is the rotation of the ellipse from the x axis as calculated in Section III. By applying R_{ψ_2} to (1), the resulting parametric equation for the ellipse becomes

$$\begin{aligned} x - x_0 &= a\cos(t) \\ y - y_0 &= b\sin(t) \end{aligned}. \tag{7}$$

The partial derivatives of these equations with respect to time are

$$\begin{aligned} \frac{\partial x}{\partial t} &= -a\sin(t), \\ \frac{\partial y}{\partial t} &= b\cos(t). \end{aligned}$$

If the MAV lies on the ellipse, its desired heading is tangent to the curve. Thus the commanded heading for the MAV, ψ^c, is given by

$$\tan(\psi^c) = \frac{\partial y}{\partial x} = \frac{\frac{\partial y}{\partial t}}{\frac{\partial x}{\partial t}} = \frac{b\cos(t)}{-a\sin(t)}. \tag{8}$$

To eliminate the parameter t from (8) we can solve (7) for $\cos(t)$ and $\sin(t)$, yielding

$$\tan(\psi^c) = \frac{b^2(x - x_0)}{-a^2(y - y_0)}.$$

If the MAV is not on the desired elliptical orbit, then the commanded heading must be modified. The position error can be written as

$$1 - \frac{(x - x_0)^2}{a^2} - \frac{(y - y_0)^2}{b^2} = error.$$

Whether the MAV is on or off of the elliptical orbit, its desired heading is calculated using

$$\begin{aligned} \partial y &= -b^2(x - x_0) \\ &\quad + \tfrac{k(y-y_0)}{a}\left(1 - \tfrac{(x-x_0)^2}{a^2} - \tfrac{(y-y_0)^2}{b^2}\right) \\ \partial x &= a^2(y - y_0) \\ &\quad + \tfrac{k(x-x_0)}{a}\left(1 - \tfrac{(x-x_0)^2}{a^2} - \tfrac{(y-y_0)^2}{b^2}\right) \end{aligned}$$

and

$$\psi^c = \tan^{-1}\left(\frac{\partial y}{\partial x}\right) + \psi_2, \tag{9}$$

where ψ_2 is the rotation of the ellipse from the x-axis, ψ^c is the commanded heading for the MAV, and k is a gain used to tune the resulting vector field.

The left plot in Figure 6 shows a vector field for an elliptical orbit as described by (9). The right plot in Figure 6 shows a simulation of the MAV entering and tracking an elliptical orbit using the vector field approach. In this simulation, the MAV starts in the center of the ellipse, enters the elliptical orbit, and executes a complete orbit. The MAV tracks the orbit to within one meter, as shown in Figure 7.

B. Longitudinal Control

The longitudinal control of the MAV is used to match the altitude of the MAV to that of the drogue. The commanded altitude for the MAV is the altitude of the drogue at its current position. The autopilot calculates a desired angle of attack for the MAV using a PID controller. In simulation, the altitude of the MAV matches the altitude of the drogue to within one meter for an entire orbit, as shown in Figure 7.

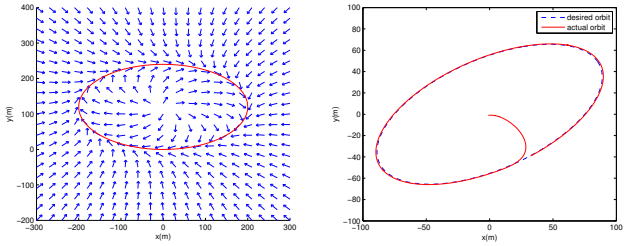

Fig. 6. Left Plot: Vector field for an elliptical orbit. Right plot: Elliptical orbit tracking. The dashed line represents the drogue orbit, and the solid line represents the MAV trajectory as it tracks the desired orbit, starting from an initial position at the center of the orbit.

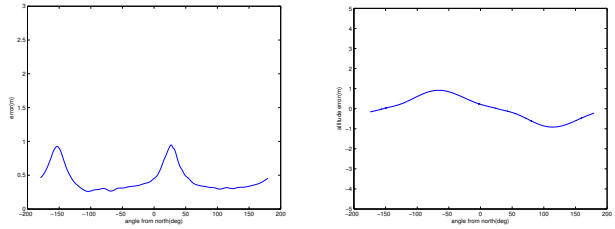

Fig. 7. Error in tracking an elliptical orbit for a single orbit. Also, altitude error for MAV tracking the drogue during an elliptical orbit. The error is consistently less than 1 m for all both plots.

V. Conclusion and Future Work

In this paper, essential methods to enable aerial recovery of micro air vehicles have been proposed. The methods allow an autonomous MAV to estimate the elliptical orbit of a recovery drogue, and then track the drogue's orbit up until the point in which final docking occurs. The methods for ellipse estimation have been shown through simulation to robustly estimate arbitrarily rotated ellipses. A RLS algorithm provides updated estimates to refine the initial estimate as new GPS data is made available to the MAV. A decoupled orbit tracking algorithm, based on vector fields, has also been demonstrated.

Ongoing work seeks to address the key limitation of the RLS algorithm, i.e., that the solution is not guaranteed to be an ellipse. The initial orbit estimate is forced to be an ellipse using the methods described in Section II-B, but once the RLS algorithm takes over, the solution may evolve into some other conic. By using a Kalman filter with nonlinear state constraints, the solution can be projected onto the space where the ellipse-specific constraint is satisfied [15], [16]. Optimal insertion of the MAV into the drogue orbit to avoid collision is being investigated, following the methods described by McLain and Beard [17] and Kingston and Beard [18]. This addition will introduce a phase into the control law that describes the position of the drogue in the orbit. Their work also extends to involve multiple MAVs, which may be applicable in future work involving multiple MAVs docking with the same drogue.

The algorithms used for orbit tracking currently result in some steady state error. In order to eliminate this error, a feed forward term will be added to the control. In order to take advantage of the out of plane estimation, we are also seeking to develop a 3D guidance law instead of decoupling the control into separate lateral and longitudinal algorithms.

Vision-based proportional navigation will be added in future work for the final phase of docking [7]. As in previous work, the methods and algorithms will be validated and refined through flight tests.

VI. Acknowledgments

This research was supported by the Air Force Office of Scientific Research under STTR contract No. FA 9550-09-C-0102 to Procerus Technologies and Brigham Young University.

References

[1] R. A. Skop and Y. Choo, "The configuration of a cable towed in a circular path," *Journal of Aircraft*, vol. 8, pp. 856–862, 1971.

[2] J. J. Russel and W. J. Anderson, "Equilibrium and stability of a circularly towed cable subject to aerodynamic drag," *Journal of Aircraft*, vol. 14, no. 7, pp. 680–686, 1977.

[3] P. Williams and P. Trivailo, "Dynamics of circularly towed cable systems, part 1: Optimal configurations and their stability," *AIAA Journal of Guidance, Control, and Dynamics*, vol. 30, pp. 753–765, 2007.

[4] P. Williams and P. Trivailo, "Dynamics of a circularly towed cable systems, part 2: Transitional flight and deployment control," *AIAA Journal of Guidance, Control, and Dynamics*, vol. 30, pp. 766–779, 2007.

[5] R. M. Murray, "Trajectory generation for a towed cable flight control system," in *13th Triennial World Congress of the International Federation of Automatic Control*, pp. 395–400, 1996.

[6] L. Sun, R. W. Beard, M. B. Colton, and T. W. McLain, "Dynamics and control of cable-drogue system in aerial recovery of mirco air vehicles based on gauss's principle," in *Proceedings of the 2009 American Control Conference*, pp. 4729–4734, June 2009.

[7] R. W. Beard, J. W. Curtis, M. Eilders, J. Evers, and J. R. Cloutier, "Vision aided proportional navigation for micro air vehicles," in *AIAA Guidance, Navigation, and Control Conference and Exhibit*, August 2007.

[8] M. Colton, S. Sun, D. Carlson, and R. Beard, "Multi-vehicle dynamics and control for aerial recovery of mcro air vehicles." To Be Published in International Journal of Vehicle Autonomous Systems, 2010.

[9] A. Fitzgibbon, M. Pilu, and R. B. Fisher, "Direct least square fitting of ellipses," *IEEE Transactions: Pattern Analysis and Machine Intelligence*, vol. 21, pp. 476–480, 1999.

[10] W. Gander, "Least squares with a quadratic constraint," *Numerische Mathematik*, vol. 36, pp. 291–307, 1981.

[11] R. Halir and J. Flusser, "Numerically stable least squares fitting of ellipses," in *Proceedings of the 6th International Conference in Central Europe on Computer Graphics and Visualization*, 1998.

[12] T. K. Moon and W. C. Sterling, *Mathematical Methods and Algorithms*. Prentice Hall, 2000.

[13] H. Baruh, *Analytical Dynamics*. WCB/McGraw-Hill, 1999.

[14] D. B. Barber, S. R. Griffiths, T. W. McLain, and R. W. Beard, "Autonomous landing of miniature aerial vehicles," *AIAA Journal of Aerospace Computing, Information, and Communication*, vol. 4, pp. 70–84, May 2007.

[15] D. Simon and T. L. Chia, "Kalman filtering with state equality constraints," *IEEE Transactions on Aerospace and Electronic Systems*, vol. 38, pp. 128–136, January 2002.

[16] C. Yang and E. Blasck, "Kalman filtering with nonlinear state constraints," in *2006 9th International Conference on Information Fusion*, July 2006.

[17] T. W. McLain and R. W. Beard, "Coordination variables, coordination functions, and cooperative-timing missions," *AIAA Journal of Guidance, Control, and Dynamics*, vol. 27, pp. 150–161, July 2004.

[18] D. B. Kingston and R. W. Beard, *Advances in Cooperative Control and Optomization*, ch. UAV Splay State Configuration for Moving Targets in Wind. Springer Berlin, 2007.